Available online at www.sciencedirect.com
ScienceDirect
Surface Science 600 (2006) 4622–4632
SURFACE SCIENCE
www.elsevier.com/locate/susc

Oxygen adsorption and oxidation reactions on Au(2 1 1) surfaces: Exposures using O_2 at high pressures and ozone (O_3) in UHV

Jooho Kim [a], Enrique Samano [b], Bruce E. Koel [a,*]

[a] Department of Chemistry, Lehigh University, 6 E. Packer Avenue, Bethlehem, PA 18015-3172, United States
[b] Centro de Ciencias de la Materia Condensada, Universidad Nacional Autónoma de México, Ensenada, BC, Mexico

Received 1 March 2006; accepted for publication 26 July 2006
Available online 28 August 2006

Abstract

Nanosized gold particles supported on reducible metal oxides have been reported to show high catalytic activity toward CO oxidation at low temperature. This has generated great scientific and technological interest, and there have been many proposals to explain this unusual activity. One intriguing explanation that can be tested is that of Nørskov and coworkers [Catal. Lett. 64 (2000) 101] who suggested that the "unusually large catalytic activity of highly-dispersed Au particles may in part be due to high step densities on the small particles and/or strain effects due to the mismatch at the Au-support interface". In particular, their calculations indicated that the Au(2 1 1) stepped surface would be much more reactive towards O_2 dissociative adsorption and CO adsorption than the Au(1 1 1) surface. We have now studied the adsorption of O_2 and O_3 (ozone) on an Au(2 1 1) stepped surface. We find that molecular oxygen (O_2) was not activated to dissociate and produce oxygen adatoms on the stepped Au(2 1 1) surface even under high-pressure (700 Torr) conditions with the sample at 300–450 K. Step sites do bind oxygen adatoms more tightly than do terrace sites, and this was probed by using temperature programmed desorption (TPD) of O_2 following ozone (O_3) exposures to produce oxygen adatoms up to a saturation coverage of $\theta_O = 0.90$ ML. In the low-coverage regime ($\theta_O \leqslant 0.15$ ML), the O_2 TPD peak at 540 K, which does not shift with coverage, is attributed to oxygen adatoms that are bound at the steps on the Au(2 1 1) surface. At higher coverages, an additional lower temperature desorption peak that shifts from 515 to 530 K at saturation coverage is attributed to oxygen adsorbed on the (1 1 1) terrace sites of the Au(2 1 1) surface. Although the desorption kinetics are likely to be quite complex, a simple Redhead analysis gives an estimate of the desorption activation energy, E_d, for the step-adsorbed oxygen of 34 kcal/mol and that for oxygen at the terraces near saturation coverage of 33 kcal/mol, values that are similar to others reported on Au surfaces. Low Energy Electron Diffraction (LEED) indicates an oxygen-induced step doubling on the Au(2 1 1) surface at low-coverages ($\theta_O = 0.08$–0.17 ML) and extensive disruption of the 2D ordering at the surface for saturation coverages of oxygen ($\theta_O \geqslant 0.9$ ML). Overall, our results indicate that *unstrained* step sites on Au(2 1 1) surfaces of dispersed Au nanoparticles do not account for the novel reactivity of supported Au catalysts for CO oxidation.

Keywords: Gold; Au(2 1 1); Stepped surface; Adatoms; Chemisorption; Ozone; Oxygen; Gold oxidation; Temperature programmed desorption (TPD); Low energy electron diffraction (LEED)

1. Introduction

Gold is the noblest metal and has limited activity for chemisorption of organic molecules [1]. Nonetheless, nanosized gold particles supported on reducible metal oxides apparently show high catalytic activity toward CO oxidation at low temperature [2–17]. Thus, it is of interest to investigate the fundamental surface science of reactions of oxygen on Au. Such studies have been limited because O_2 does not chemisorb on Au surfaces under normal ultrahigh vacuum (UHV) conditions, but Au can be oxidized by O_3

* Corresponding author. Tel.: +1 610 758 5650; fax: +1 610 758 6555.
E-mail address: brk205@lehigh.edu (B.E. Koel).

0039-6028/$ - see front matter © 2006 Elsevier B.V. All rights reserved.
doi:10.1016/j.susc.2006.07.057

(ozone) [18–20], or other aggressive methods including O_2 dissociation by a hot filament [21–24], microwave-excited O_2 dosing [25,26], oxygen reactive sputtering [27–29], exposure to an O_2 plasma [30,31], and electron-induced dissociation of condensed layers of NO_2 [32,33] or O_2 [34,35].

Although there were some early reports of gold oxide formed on Au single crystals in UHV, Schrader [36] observed that surface-segregated calcium could cause strongly bound oxygen chemisorption above 600 °C. Eley and Moore [37] reported that very little oxygen could be chemisorbed on polycrystalline gold foil at less than 1000 K with $P(O_2) < 5 \times 10^{-5}$ Torr. Legaré et al. [38] investigated O_2 adsorption on Au(1 1 1) and polycrystalline Au foil over temperatures from 25 to 850 °C and O_2 pressures from 10^{-8} to 10 Torr. Even though no oxygen species was found at 25 °C for all pressures studied, oxygen could be adsorbed above 300 °C and calcium enhanced oxygen adsorption on both surfaces. Those contradictions were explained by Pireaux et al. [39] who reported that O_2 did not dissociatively adsorb on gold surfaces under UHV conditions unless there were impurities (Ca, Mg, and Si) present. This explanation was confirmed by Canning et al. [23].

Sault et al. [22] investigated O_2 adsorption on the Au(1 1 0)-(1 × 2) surface using O_2 pressures up to 1400 Torr and temperatures from 300 to 500 K. No O_2 dissociative adsorption was detected. Using O_2 dissociation over a hot filament, they obtained a 0.95-ML coverage of oxygen adatoms. Recombinative O_2 desorption took place to give a peak in TPD at 590 K, which corresponds to a desorption activation energy of 32 kcal/mol Recently, O_2 adsorption on the Au(1 1 0)-(1 × 2) surface between 28 and 700 K was studied by Gottfried et al. [34] using several surface analytical techniques. Molecular adsorption of O_2 occurred at 28 K. Peaks in TPD were observed for O_2 desorption at 51 and 45 K from the first layer (with a coverage of 0.30 ML O_2), 37 K from the second layer, and 34 K from the multilayer. The binding energy of adsorbed O_2 was estimated to be less than 3 kcal/mol. O_2 adsorption was accompanied by a decrease in the work function of 0.22 eV upon completion of the first adsorbed layer. Ultraviolet photoelectron spectroscopy (UPS) and near-edge X-ray absorption fine structure spectroscopy (NEXAFS) showed typical signals for physisorbed O_2 layers at monolayer coverage on the surface. Oxygen adatoms were generated on the surface by ultraviolet (UV) irradiation and electron bombardment. Chemisorbed oxygen ($\theta_O < 0.20$ ML) desorbed above 500 K with second-order kinetics and a desorption activation energy of 33 kcal/mol. An additional O_2 TPD peak at 490 K occurred above monolayer coverage, and this was attributed to decomposition of gold oxide.

In addition, Gottfried et al. [40] reported oxidation of gold by oxygen-ion sputtering. From these surfaces, peaks in O_2 TPD curves occurred between 350 and 950 K. Oxygen desorption at 415 K with $E_d = 25$ kcal/mol was assigned to gold oxide decomposition and desorption at 545 and 620 K with $E_d = 38$ kcal/mol was assigned to recombination of chemisorbed oxygen. An O_2 TPD peak at 850 K with $E_d = 49$ kcal/mol was attributed to oxygen atoms dissolved in the bulk. During oxygen-ion sputtering, higher ion energies (5 keV, 3 μA/cm^2) favored occupation of bulk sites while lower energies (1 keV, 1 μA/cm^2) formed chemisorbed oxygen and gold oxide at the surface. Previous reports of oxygen desorption at temperatures above 600 K could be explained by oxygen in bulk sites.

O_2 does not dissociatively adsorb on Au(1 1 1) under UHV conditions [19,20], however, Friend and coworkers [32] have recently reported that the presence of oxygen on the reconstructed Au(1 1 1) surface increased the O_2 dissociation probability by several orders of magnitude. In studies using ozone to produce oxygen adatoms with coverages up to 1.2 ML, O_2 desorption from Au(1 1 1) was described by first-order kinetics with an activation energy of 30 kcal/mol near saturation coverage [19,20]. All oxygen was removed by thermal desorption of O_2 to leave a clean Au(1 1 1) surface after heating to 600 K.

King reported oxidation of polycrystalline gold films that were exposed to UV/ozone in laboratory air [41]. A gold oxide layer was formed that was 17 ± 4 Å thick with an initial stoichiometry of Au_2O_3. Another study using X-ray photoelectron spectroscopy (XPS) of (1 1 1)-textured Au films exposed to UV/ozone found 0.8-ML adsorbed oxygen and a few-ML thick gold oxide with a stoichiometry close to Au_2O_3 [42]. Both oxygen states disappeared when heated to 150–200 °C. In addition, Koslowski et al. [30] investigated the oxidation of preferentially (1 1 1)-oriented Au films in an oxygen plasma. The surface was oxidized to a depth of 4 nm, leading to a rough surface morphology. The gold surface was fully reduced by heating to 200 °C.

A consistent picture of O_2 chemistry on Au has emerged from all of this work, one in which it is nearly impossible to activate dissociative O_2 adsorption on any metallic bulk gold surface. Of course, nanometer-sized particles of Au might be expected to have different chemistry than bulk Au (recent experimental results by Kim et al. [43] show that Au atoms deposited directly onto an O_2 multilayer at 22 K can dissociate O_2 molecules to form Au–O clusters), and it is conceivable that steps, defects, or special crystal planes that are exposed and stabilized on such nanoparticles might explain the novel properties reported for nanometer-sized particles of Au. Indeed, Nørskov and coworkers [44] suggested that the "unusually large catalytic activity of highly-dispersed Au particles may in part be due to high step densities on the small particles and/or strain effects due to the mismatch at the Au-support interface". They concluded that oxygen adatoms were bound stronger on the stepped Au(2 1 1) surface than on the flat Au(1 1 1) surface based on calculations of the dissociative O_2 and molecular O_2 adsorption energies. More importantly, they also concluded that the barrier for O_2 dissociation was lower at the steps regardless of whether O_2 dissociation occurred at the steps or on the support. This would lead to a higher CO oxidation rate in the vicinity of steps because the concentration of oxygen adatoms would be increased due to the lower barrier for O_2 dissociation.

Xu and Mavrikakis [45] recently recalculated the molecular and atomic oxygen binding energies on the Au(1 1 1) and Au(2 1 1) surfaces, along with the O_2 dissociation energy barriers. Their results indicate that molecular O_2 does not adsorb on the Au(1 1 1) surface while it does adsorb weakly on the Au(2 1 1) surface with $E_{ads} = 3.6$ kcal/mol. They calculate that the binding energy of atomic oxygen is 58.6 kcal/mol on Au(1 1 1) and 63.9 kcal/mol on Au(2 1 1). They report activation barriers for O_2 dissociation on stretched (10%) and unstretched Au(2 1 1) of $E^{diss} = 14.5$ and 25.8 kcal/mol, respectively. These barriers are much smaller than on a stretched Au(1 1 1) surface, $E^{diss} = 31.6$ kcal/mol. And so, even though O_2 dissociation is an activated process on gold, they conclude that "steps and tensile strain substantially facilitate O_2 activation on Au surfaces". Another calculation of the O_2 dissociation barrier on Au surfaces by Liu and Hu [46] found that O_2 does not dissociate on Au(2 1 1) because of a high barrier, $E^{diss} = 21.4$ kcal/mol, although this is lower than $E^{diss} = 51.4$ kcal/mol on Au(1 1 1). They also propose that O_2 dissociation on Au surfaces, including Au particles, does not occur at low temperatures.

We reported herein results of our investigations of aspects of oxygen chemistry on a particular stepped surface, Au(2 1 1). The clean Au(2 1 1) surface has a structure in which three-atom wide terraces with local (1 1 1) orientation are separated by monatomic steps with (1 0 0) orientation [47]. O_2 was exposed on the Au(2 1 1) surface from UHV conditions up to high pressures (700 Torr) using an attached high-pressure reaction cell, and we also investigated ozone dosing under UHV conditions. Auger electron spectroscopy (AES), low energy electron diffraction (LEED), temperature program desorption (TPD) and infrared reflection–absorption spectroscopy (IRAS) were used to characterize these surfaces.

2. Experimental methods

Experiments were conducted in a two-level stainless steel UHV chamber that has been described previously [48]. The system had a base pressure of 2×10^{-10} Torr. The lower level was equipped for AES, TPD, and LEED studies, and the upper level provided capabilities for Ar^+-ion sputtering, IRAS, and high-pressure kinetics studies in an attached batch reactor cell [49]. For high-pressure studies, two Baratron gauges (Type 122A) were connected to the reaction cell to measure pressure over the range of 1 mTorr to 1000 Torr.

A Au(2 1 1) crystal (Metal Crystal & Oxides, LTD, 10-mm dia., 2-mm thick) was mounted using two 0.015 in.-dia. W wires attached to two 0.126 in.-dia. Ta rods that were pressed into a liquid-nitrogen cooled Cu block. The crystal could be heated resistively to 1100 K and cooled to 85 K as monitored by a chromel–alumel thermocouple pressed firmly (using Au foil) into a small hole in the side of the crystal. The crystal was cleaned by repeated cycles of Ar^+-ion sputtering (500 eV, 2 μA) for 10 min with the sample at 300 K and annealing at 985 K for 10 min in UHV. This procedure was repeated until the carbon peak in AES ($E_p = 3$ keV) did not decrease further ($\theta_c < 0.02$ ML). After this, the crystal was exposed to 1×10^{-5}-Torr O_2 for 5 min with the sample temperature at 873 K and flashed to 985 K for 1 min. After this initial, extensive cleaning procedure, only limited sputtering was needed and exposure to 1×10^{-5}-Torr O_2 at 873 K for 5 min and flashing the surface to 985 K for 1 min was sufficient to remove any small carbon signal in AES.

High-purity O_2 was used in the high-pressure experiments (Matheson Gas Products, UHP grade, 99.998% purity) without further purification. Ozone used for dosing in UHV was prepared in our laboratory using a commercial ozone generator as described elsewhere [20].

TPD experiments were performed with the crystal in line-of-sight of the ionizer of the quadrupole mass spectrometer (QMS) and with a heating rate of 3 K/s. QMS signals at $m/e = 18$, 28, 32 and 44 were monitored simultaneously. IRAS spectra were obtained by using a Mattson Infinity 60MI spectrometer operated at 4 cm^{-1} resolution and accumulating 1000 scans for each spectrum [50].

Absolute coverages are used throughout this paper referenced to the Au surface atom density such that $\theta = 1.0$ ML corresponds to 1.48×10^{15} atoms/cm^2.

3. Results and discussion

3.1. Structure of the Au(2 1 1) surface

The LEED pattern that we obtained from a clean Au(2 1 1) surface is shown in Fig. 1(a). The unit cell characterizing this pattern is shown as a white rectangle superimposed on the photograph. This pattern can be simply understood by describing the Au(2 1 1) surface in a microfacet notation denoted as $3(1\,1\,1) \times (1\,0\,0)$, i.e., a step-terrace structure consisting of three-atom wide terraces of (1 1 1) orientation and a monatomic step with a (1 0 0) orientation. Schematic drawings of this real-space structure of the Au(2 1 1) surface are shown in Fig. 1(b) in side-view and (c) in top-view. The rectangle in the lower right corner of Fig. 1(c) indicates the primitive surface unit cell with a size of 7.05×2.88 Å. Thus, the distance between LEED spots along the $[\bar{1}\,1\,1]$ direction is one-third of the distance between first-order spots from the (1 1 1) terraces because the step is separated by three-atom wide (1 1 1) terraces. Overall, the hexagonal pattern is from the (1 1 1) structure of the terraces.

3.2. Exposures using O_2 in UHV on the Au(2 1 1) surface

A wide range of exposures of oxygen (O_2) was dosed on the Au(2 1 1) surface at several different temperatures of 85, 300, 400 and 450 K under UHV conditions. All but the largest exposures produced no measurable adsorption of any gases on the surface at any temperature. We show one set of TPD curves in Fig. 2 obtained after the largest

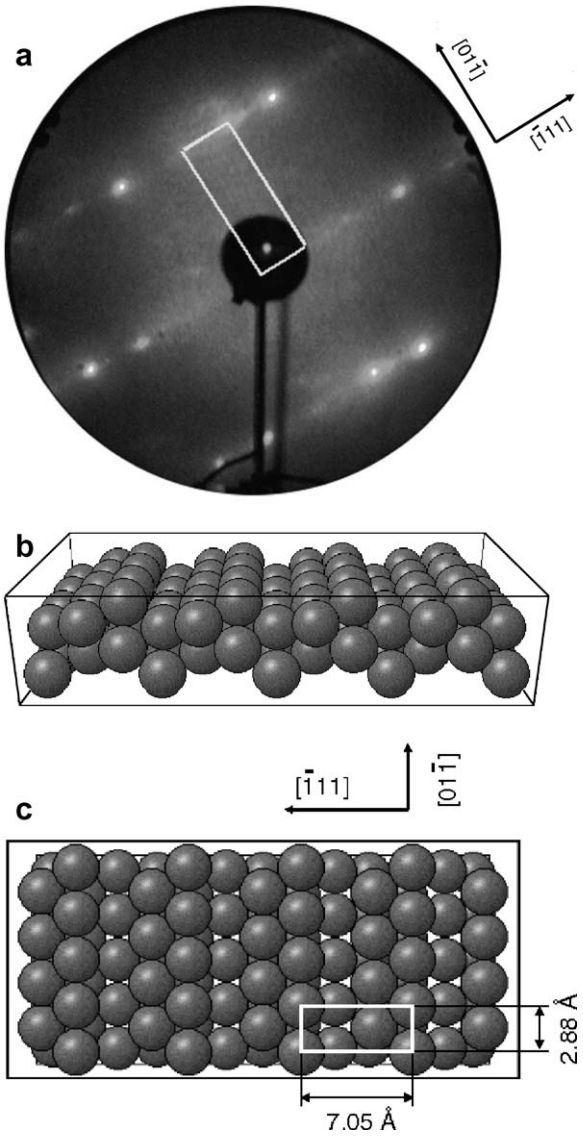

Fig. 1. Structure of the Au(2 1 1) surface. (a) Photograph of the LEED pattern from the Au(2 1 1) surface obtained at a beam energy of 75 eV. (b) Side view and (c) top view of real-space schematic drawings of the Au(2 1 1) surface. The superimposed white rectangular box in (a) and (c) represents the unit cell of the Au(2 1 1) surface. The size of the unit cell is 7.05×2.88 Å.

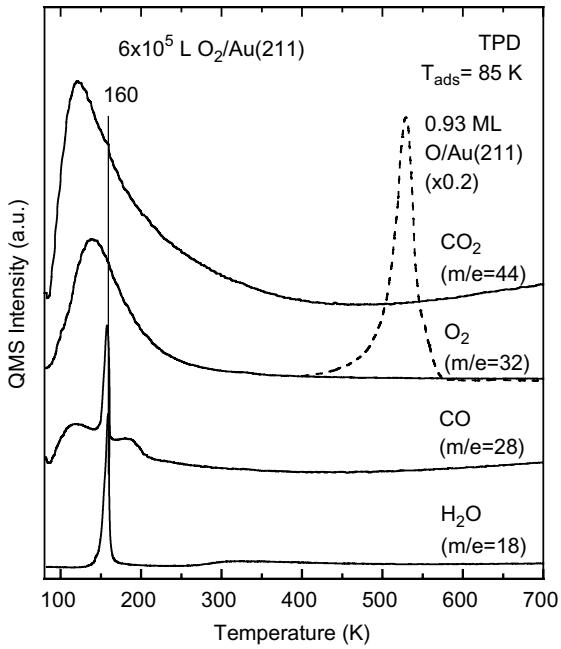

Fig. 2. TPD curves after a 6×10^5-L O_2 exposure on Au(2 1 1) at 85 K. The dashed line provides the O_2 TPD curve obtained from 0.9-ML O/Au(2 1 1) for comparison. The absence of a discernable peak above 500 K at $m/e = 32$ indicates that oxygen adatoms were not formed on the Au(2 1 1) surface by O_2 exposures.

exposure that we utilized of 6×10^5-L O_2 on Au(2 1 1) at 85 K. This exposure was carried out using a stainless steel doser that provided direct line-of-sight dosing onto the Au(2 1 1) crystal face under conditions of 1×10^{-3}-Torr O_2 for 600 s with the ion gauge and ion pump turned off to avoid production of excited oxygen species (dynamic pumping was maintained by a 230 l/s turbomolecular pump). The subsequent TPD spectrum showed no detectable O_2 desorption peak near 530 K. For comparison, we show in this figure the O_2 TPD peak (dashed curve) produced from 0.9 ML of oxygen adatoms formed by ozone (O_3) exposure (as discussed below) on Au(2 1 1). Thus, O_2 does not dissociatively adsorb on the Au(2 1 1) surface at any temperature between 85 and 450 K under UHV conditions. Such a large exposure understandably produces contaminant water coadsorption and desorption at 160 K [51] and large "background" effects due to desorption from surfaces other than the Au(2 1 1) crystal face that produce broad peaks near 120 K. The sharp CO TPD peak at 160 K arises from coadsorbed CO that is trapped on the surface until the water multilayer desorption occurs.

AES spectra (not shown here) that were obtained following exposures of 6×10^5-L O_2 on Au(2 1 1) at 300, 400 and 450 K did not detect any oxygen on the surface. AES spectra obtained after dosing on the crystal at 85 K showed a small oxygen signal, but we associate this with the coadsorbed water and CO that was identified using TPD.

We also carried out additional O_2 dosing experiments on a Au(2 1 1) surface that had been atomically roughened by 500-eV Ar^+-ion sputtering at 300 K without annealing the surface to any higher temperature. The results were the same as those discussed above and no detectable reactivity was observed.

In addition, infrared reflection–absorption spectroscopy (IRAS) was used to probe the Au(2 1 1) surface after these O_2 exposures. IR spectra obtained from Au clusters deposited in a O_2/Ar matrix at 10 K have been used previously to identify a Au–O_2 complex based on a vibrational band at 1092 cm^{-1} [52]. We did not observe any vibrational bands that we felt comfortable assigning to physisorbed or chemisorbed O_2 species on the Au(2 1 1) surface under any of the conditions discussed above. Specifically, IRAS spectra that were obtained following an exposure of 6×10^5-L O_2 on

Au(2 1 1) at 85 K, and after the surface was annealed sequentially to 150, 180, 240 and 300 K and then re-cooled to 85 K [49], showed only bands that we associated with condensed water and coadsorbed CO on the surface.

3.3. Exposures using O_2 at high pressures (~1 atm) on the Au(2 1 1) surface

O_2 could be exposed on the Au(2 1 1) surface at pressures up to 1 atm by utilizing the high-pressure reactor cell that was attached to the UHV chamber. This antechamber is normally open directly to the UHV environment and thus is maintained in a relatively clean and evacuated condition prior to isolation and pressurization. A number of high-pressure O_2 experiments were carried out using the following procedure. The clean Au(2 1 1) crystal at 300 K or above was isolated from UHV in the reactor cell by closing a $2-3/4$ in. OD gate valve. The cell was then pressurized at up to 700 Torr of O_2. Experiments with the crystal at elevated temperatures of 400 and 450 K were carried out by first heating the crystal to temperature in the high-pressure gas and then cooling the crystal back to 300 K prior to evacuation. A number of O_2-exposure experiments over the pressure range of 1–700 Torr O_2 were performed with the Au(2 1 1) surface at 300, 400 and 450 K. Fig. 3 shows data from one set of such experiments in which AES spectra were obtained following exposure of 700-Torr O_2 for 5 min on the Au(2 1 1) surface at 300–450 K. We conclude, based on these results, that the amount of oxygen uptake on the Au(2 1 1) surface from these high-pressure O_2 exposures was clearly less than $\theta_O \leqslant 0.07$ ML, and we always have to be concerned about contamination issues when observing such a small amount. This value for the maximum oxygen coverage was obtained by comparing the O(517 eV)/Au(240 eV) AES peak-to-peak height ratio with the calibration determined in a previous study in our group [20]. The small carbon AES signal at 272 eV kinetic energy (KE), estimated to be $\theta_C \leqslant 0.3$ ML based on our experience, understandably arises from hydrocarbon contamination from such high-pressure conditions and is not sufficient to affect our results substantially.

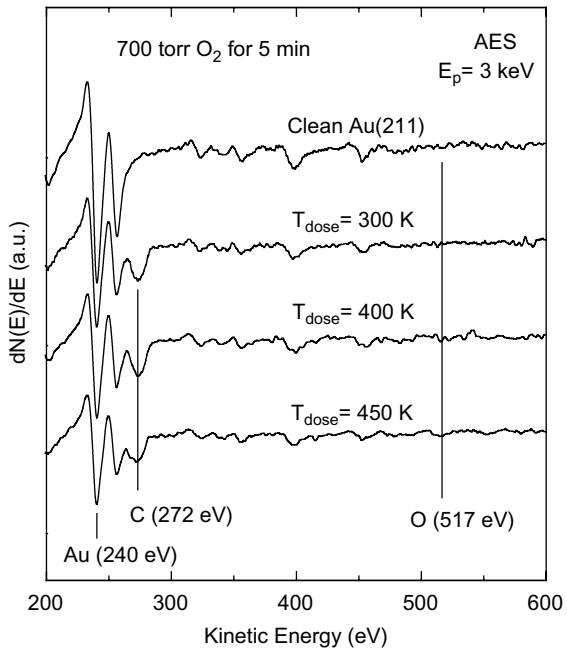

Fig. 3. AES spectra obtained after high pressure O_2 exposures (700 Torr, 5 min) of the Au(2 1 1) surface at 300, 400 and 450 K. Submonolayer amounts of carbon from hydrocarbon contamination were observed in some cases at the highest pressure conditions.

Given our previous results on Au(1 1 1) surfaces showing a high CO reaction probability with oxygen adatoms [19], we were concerned about the possibility that oxygen adatoms formed by O_2 dissociation under high-pressure conditions could be titrated by the small concentration of CO present as an impurity in the high-pressure gas, making it appear that no O_2 dissociation occurred. Although it does not completely prove that reductant contamination is not a problem, we carried out the following control experiment. The Au(2 1 1) surface was first precovered by oxygen adatoms with $\theta_O = 0.15$ ML in the UHV chamber by using the hot filament of the QMS and then subsequently placed within the high-pressure reactor and exposed to 10-Torr O_2 for 20 min at 300 K. After removing the Au(2 1 1) crystal from the reactor cell, AES showed a decrease in the oxygen AES signal equivalent to 0.05 ML, or 35% of the initial oxygen coverage. This indicates that the rate of O_2 dissociation to produce surface-bound oxygen is smaller than the rate of surface reduction by CO that results from the trace contamination in the cell from high-pressure O_2. This indicates that CO reduction would only decrease the apparent extent of oxygen uptake, but not eliminate evidence for it, and so the Au(2 1 1) surface at 300–450 K is quite unreactive for O_2 dissociation.

One can calculate a lower limit on the dissociation activation energy barrier E^{diss} on the Au(2 1 1) surface from the high-pressure O_2 exposure given in these experiments. Consider that O_2 dissociative adsorption occurs via the following elementary reaction steps:

$$O_2(g) \underset{k_d}{\overset{k_{ad}}{\rightleftarrows}} O_2(ad) \tag{1}$$

$$O_2(ad) \overset{k_{diss}}{\rightarrow} 2O(ad) \tag{2}$$

The adsorption rate, R_{ad}, in reaction 1 is given by

$$R_{ad} = k_{ad}(P_{O_2}) \tag{3}$$

where k_{ad} is the adsorption rate constant. The desorption rate, R_d, in Eq. (1) is given by

$$R_d = \frac{d[O_2(ad)]}{dt} = -k_d[O_2(ad)] \tag{4}$$

where k_d is desorption rate constant. The O_2 dissociation rate, R_{diss}, in Eq. (2) can be written as

$$R_{diss} = \frac{d[O(ad)]}{dt} = 2k_{diss}[O_2(ad)]f(\theta) \tag{5}$$

where $f(\theta)$ is a structure factor involving the coverage θ, which here is given by $(1-\theta_o)^2$ since two adjacent empty sites on the surface are needed for dissociation, and k_{diss} is the dissociation rate constant. Using a steady-state approximation, which assumes that the concentration of the O_2(ad) intermediate does not change significantly during the reaction, we can write

$$[O_2(ad)] = \frac{k_{ad}}{k_d + k_{diss} f(\theta)} (P_{O_2}) \quad (6)$$

Substituting this expression for $[O_2(ad)]$ into Eq. (5) and assuming that for the pre-exponential factors $v_d = v_{diss}$, we can now write a final, general expression for dissociative adsorption as

$$R_{diss} = \frac{d[O(ad)]}{dt} = 2\frac{1}{\sqrt{2\pi m k_B T}} \exp\left(-\frac{E_{ads}}{RT}\right) \times \frac{1}{\frac{1}{f(\theta)} \exp\left(\frac{-E_d + E^{diss}}{RT}\right) + 1} (P_{O_2}) \quad (7)$$

where E_{ads} is the barrier to molecular O_2 adsorption, and E_d is the O_2 desorption activation energy. It is safe to assume that $E_{ads} = 0$ because O_2 is only weakly physisorbed on the Au surface, and so when we solve Eq. (6) for E^{diss} we find

$$E^{diss} = E_d + RT \ln\left(\frac{f(\theta)(P_{O_2})}{R_{diss}} \cdot \frac{2}{\sqrt{2\pi m k_B T}} - f(\theta)\right) \quad (8)$$

This equation can be used to estimate E^{diss} by utilizing the parameters of the experiment along with a value for E_d. This latter value can be calculated from O_2 TPD data in which $T_p = 45$ K [34,43], indicating that $E_d = 2.7$ kcal/mol (from Redhead analysis, first order desorption, and $v = 10^{13}$ s^{-1}). Finally, we calculate an upper limit on the value of R_{diss} by assuming that the oxygen coverage of 0.07 ML found after high-pressure O_2 exposure with $P_{O_2} = 700$ Torr for 5 min with the substrate at 450 K was created from dissociative O_2 adsorption (and not from any contamination reaction), then $R_{diss} < (0.07$ ML/300 s) or 2.33×10^{-4} ML s^{-1}. This rate can be converted to $R_{diss} < 3.45 \times 10^{15}$ atoms m^{-2} s^{-1} using the Au(2 1 1) surface atom density of 1.48×10^{15} atoms cm^{-2}. This calculation provides then a lower limit on the activation energy barrier for O_2 dissociation, E^{diss} of 27 kcal/mol on the Au(2 1 1) crystal surface.

Even though we could not reliably extend our measurements to include higher pressures and temperatures in order to determine a value for E^{diss}, our estimate of a lower limit establishes that this is a relatively high value and that there is no facile pathway for O_2 thermal dissociation to produce oxygen adatoms on the stepped Au(2 1 1) surface. Another experimental number available is also a lower limit for E^{diss} of 36 kcal/mol that we can calculate from the data of Sault et al. [22] investigating O_2 adsorption on the Au(1 1 0)-(1 × 2) surface using O_2 pressures up to 1400 Torr and temperatures from 300 to 500 K. We note the report of a value of 81 kcal/mol for O_2 dissociative adsorption on the Au(1 1 0)-(1 × 2) surface in Ref. [53], but the origin of this number is unclear. We can compare also to results from theoretical calculations, and we note that our lower limit is larger than those values for O_2 dissociation on stretched (10%) and unstretched Au(2 1 1) of $E^{diss} = 14.5$ and 25.8 kcal/mol, respectively [45]. Liu and Hu [46], based on other theoretical calculations, concluded that O_2 does not dissociate on Au(2 1 1) because of a high barrier, $E^{diss} = 21.4$ kcal/mol, although this was lower than their calculation of $E^{diss} = 51.4$ kcal/mol on Au(1 1 1).

3.4. Ozone (O_3) exposures on the Au(2 1 1) surface in UHV

Oxygen uptake on the Au(2 1 1) surface was investigated under UHV conditions by dosing the reactive oxidant ozone. O_2 TPD curves after various O_3 exposures on the Au(2 1 1) surface at 300 K are shown in Fig. 4. Nearly identical curves were generated by pre-annealing the surface to increasingly higher temperatures prior to taking the TPD curves following a saturation exposure of O_3 on a surface at 300 K. The O_2 TPD peak appeared initially at 540 K and did not shift with increasing oxygen coverage in the low-coverage regime ($\theta_O \leqslant 0.15$ ML). At higher coverages, additional low-temperature desorption appeared with a peak at 515 K for $\theta_O = 0.27$ ML, and this shifted to 530 K at saturation coverage. The peak at 540 K at low coverage is attributed to oxygen adatoms that are bound at the steps on the Au(2 1 1) surface, because such a high-temperature feature did not appear in O_2 TPD curves following ozone exposures on the Au(1 1 1) surface [20]. The low-temperature O_2 desorption feature is assigned to

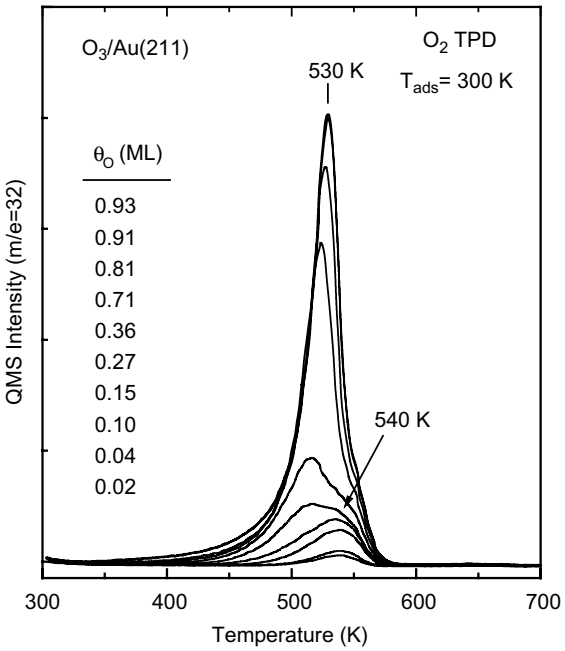

Fig. 4. O_2 TPD curves following ozone exposures on a Au(2 1 1) surface at 300 K. The peak at 540 K in the low-coverage regime ($\theta_O \leqslant 0.15$ ML) can be attributed to oxygen adsorbed on the step sites.

oxygen adsorbed on the (1 1 1) terrace sites of the Au(2 1 1) surface. This assignment is supported by the observation that this low-temperature O_2 TPD peak shifts to higher temperatures with increasing oxygen coverage as was observed for the O_2 TPD peak from the Au(1 1 1) surface [20]. Gottfried et al. [35] also observed a peak shift to higher temperatures at higher coverages on Au(1 1 0), but the low-coverage behavior was different because of the step sites on the Au(2 1 1) surface.

The uptake curve given in Fig. 5 provides the O_2 TPD peak areas from these experiments, along with values of the O(517 eV)/Au(240 eV) peak-to-peak height ratio measured from AES spectra that were taken before heating to obtain the TPD data. AES provides a method to determine the absolute oxygen coverage on the surface after saturation of the uptake. A calibration was obtained in a previous study between the O(517 eV)/Au(240 eV) AES peak-to-peak height ratio and the absolute oxygen adatom coverage [20]. Based on that calibration, we estimate that the saturation coverage from ozone dosing on the Au(2 1 1) surface at 300 K is $\theta_O = 0.90$ (± 0.04) ML. The good agreement of the AES and O_2 TPD data to provide a single uptake curve establishes that there are no loss channels for adsorbed oxygen other than O_2 desorption during TPD (e.g., diffusion of oxygen into the bulk of the Au crystal). In addition, the linear increase in the oxygen coverage with increasing ozone exposure means that the ozone dissociative sticking coefficient is constant, independent of oxygen precoverage, and ozone dissociative adsorption follows precursor-mediated adsorption kinetics.

The activation energy for O_2 thermal desorption, E_d, can be roughly estimated by using Redhead analysis [54]. For O_2 desorption in the peak at 540 K at low coverages ($\theta_O \leqslant 0.15$ ML), $E_d = 34$ kcal/mol assuming a pre-exponential factor for desorption of 1×10^{13} s^{-1} and first-order desorption kinetics. As terrace sites are populated, the value of E_d decreases to 32–33 kcal/mol at higher coverages. Recombinative O_2 desorption from oxygen adatoms at the Au(1 1 1) surface occurred in a peak that shifted from 520 to 550 K with increasing coverage, and appeared to follow first-order kinetics [20]. From the Au(1 1 1) surface, the value of E_d estimated by using Redhead analysis was 32–34 kcal/mol If one corrects for the different heating rate in Ref. [20], which was 8.5 K/s, to that used by us (3 K/s), the O_2 desorption peak temperatures of the two studies are the same at high coverages. This indicates that oxygen desorbs from similar chemical states at high coverages on the Au(2 1 1) and (1 1 1) surfaces. Oxygen desorbs from similar chemical states at low coverages on the Au(2 1 1) and (1 1 1) surfaces as well, because the temperature and values of E_d on the two surfaces are still quite close.

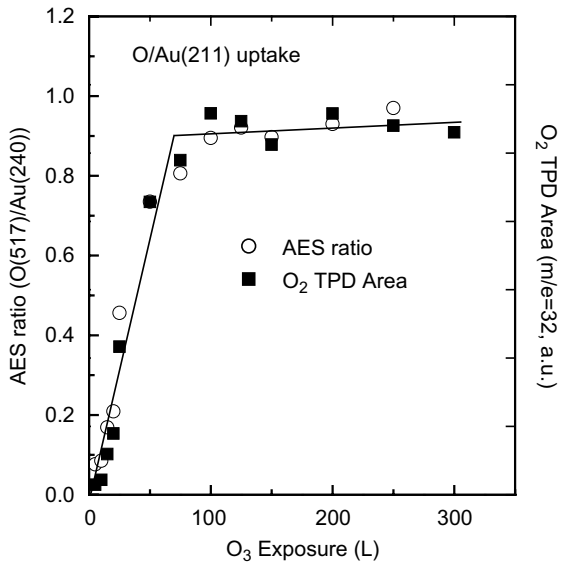

Fig. 5. Oxygen uptake curve obtained for ozone exposures on a Au(2 1 1) surface at 300 K. There is a quantitative mapping of the O(514 eV)/Au(240 eV) AES ratio to the O_2 TPD area, and so the AES ratio is directly proportional to the O coverage on the Au(2 1 1) surface.

It is of interest to try to make a better estimate of the value of E_d for O_2 desorption from the step-sites on the Au(2 1 1) surface. One can use the Polanyi–Wigner equation to determine E_d, along with values for the pre-exponential factor, ν_n and the reaction order, n [55–57]:

$$\text{Rate} = \theta^n \nu_n e^{-E_d/RT} \tag{9}$$

where θ is the coverage (ML). Taking the logarithm of both sides of Eq. (9) and rearranging yields

$$\ln R - n \ln \theta = \ln \nu_n - E_d/RT \tag{10}$$

Thus, a plot of ($\ln R - n \ln \theta$) versus ($1/T$) has a slope of $-E_d/R$ and a y-intercept of $\ln \nu_n$. Notably, this plot is only linear for the correct choice of n and if E_d and ν are not strong functions of θ. Such a plot is shown in Fig. 6 from the TPD curve for $\theta_O = 0.15$ ML in Fig. 4. The choice of $n = 1$ produces the best straight-line fit. Other choices of n gave the expected curves for incorrect choices of the reaction order, and indicates that oxygen desorption at low coverages follows apparent first-order kinetics. From this plot, E_d was calculated to be 24 kcal/mol with $\nu_1 = 2 \times 10^{14}$ s^{-1}. However, we believe that this estimate of the value of E_d for O_2 desorption from Au(2 1 1) step-sites is too low, which could arise from strong coverage dependencies of rate parameters (ν_n and E_d) and/or the much more complicated kinetics that would occur from surface restructuring and/or island dissolution. Also, other plots like that in Fig. 6 showed large changes in E_d depending on the coverage used. Thus, we prefer to estimate the increased stability of oxygen at steps versus terrace sites, which corresponds to the difference in peak temperatures of 515 versus 540 K in TPD, by using the simpler Redhead values.

Of course it would be useful if we could use the value of E_d to determine a value for the Au–O bond dissociation energy on this surface or to be able to say something about any change that occurred in the barrier for O_2 dissociative adsorption, E^{diss}, between the Au(2 1 1) and (1 1 1) surfaces. After all, in general, E_d arises from $E_{ads} + E^{diss}$, where E_{ads} is the energy for O_2 dissociative adsorption. However, in

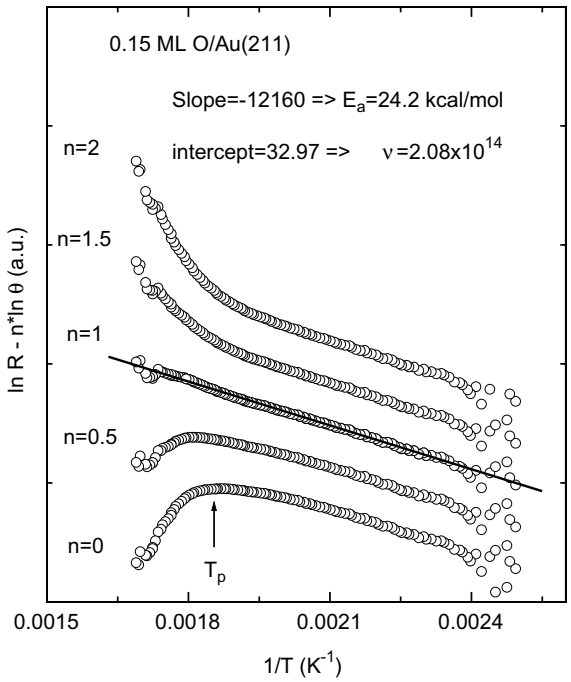

Fig. 6. O_2 TPD curves for $\theta_O = 0.15$ ML plotted according to the method of Parker et al.[56,57]. Plots for several choices of n, the desorption kinetic order, are shown, and only the data for $n = 1$ can be described well by a line in the region of $T_p = 540$ K.

this case, O_2 desorption is likely rate-limited by some other process on Au(2 1 1) and (1 1 1) surfaces, as evident by the apparent first-order desorption kinetics. This would mean that O_2 desorption kinetics are not reflecting the barrier E^{diss} and we cannot make firm conclusions about the relative sizes of E^{diss}(2 1 1) versus E^{diss}(1 1 1). Saliba et al. [20] proposed that first-order O_2 desorption kinetics on Au(1 1 1) was due to the rate-determining step in the O_2 desorption process at low coverages being the conversion of oxidic oxygen to chemisorbed oxygen. First-order kinetics observed for oxygen desorption on Au(2 1 1) at low coverages may have a similar explanation.

It is useful to compare our O_2 TPD curves to those in the previous report of Sault et al. [22] from the Au(1 1 0)-(1 × 2) surface. They assigned the low-coverage region to have second-order desorption kinetics, the mid-coverage region to have first-order kinetics, and the highest coverage region to follow zero-order kinetics. They calculated a value for E_d of 32 kcal/mol with a pre-exponential factor of 1.3×10^{12} s^{-1} at $\theta_O = 0.25$ ML. In another study of O_2 desorption from Au(1 1 0)-(1 × 2), Gottfried et al. [34] assigned second-order desorption kinetics to the lower coverages ($\theta_O \leqslant 0.25$ ML) and calculated $E_d = 34$ kcal/mol at submonolayer coverages ($\theta_O \leqslant 1.0$ ML). They also reported an additional O_2 desorption peak at 490 K for coverages higher than one monolayer and attributed this peak to the decomposition of an oxidic species. A later, more detailed investigation and analysis by these authors [35] showed very complex desorption kinetics for this system, including 'autocatalytic' desorption at coverages 0.35 ML $\leqslant \theta_O \leqslant$ 1.0 ML that shifts the desorption peak to higher temperature and narrows the width of the peak. We also mention a report of a higher O_2 desorption peak temperature of 545 K for O adatoms on >6-monolayers Au nanoparticles supported on TiO_2(1 1 0), which is qualitatively consistent with our results [24].

3.5. LEED studies of oxygen uptake from O_3 exposures on Au(2 1 1) in UHV

LEED was used to investigate the 2D ordering of the oxygen-covered Au(2 1 1) surface following O_3 exposures on Au(2 1 1) at 300 K. Photographs of the resulting LEED patterns are shown in Fig. 7. Increasing the O_3 exposure increased the coverage of oxygen on the surface as indicated below each LEED photograph. The oxygen concentration was determined by using AES as described above.

The upper left-hand picture in Fig. 7 provides a LEED pattern for the clean Au(2 1 1) surface prior to any ozone dosing. As discussed for Fig. 1, the clean Au(2 1 1) surface can be understood as a step-terrace structure consisting of three-atom wide terraces of (1 1 1) orientation and a monatomic step with a (1 0 0) orientation, or 3(1 1 1) × (1 0 0) in microfacet notation. This gives rise to an overall hexagonal LEED pattern, from the (1 1 1) structure of the terraces, but with a rectangular unit cell from LEED spots along the [$\bar{1}$ 1 1] direction at one-third of the distance between first-order spots from the (1 1 1) terraces due to separation of the steps by three-atom wide (1 1 1) terraces. In this LEED pattern, and other subsequent ones, "streaking" or extra intensity along the [$\bar{1}$ 1 1] direction was observed because of the presence of additional step separations, i.e., 3, 4, 5, ...-atom wide (1 1 1) terraces.

Fig. 7 shows that oxygen uptake to $\theta_O = 0.16$–0.24 ML proceeds without significant increases in the background intensity or spot broadening. However, new spots appear at $^1/_6$ of the distance of the first-order (1 1 1) spots, which indicates a doubling of the unit cell size of the clean surface. We interpret this to mean that oxygen uptake to $\theta_O = 0.16$–0.24 ML is localized at step sites, and this induces a "step-doubling" on the Au(2 1 1) surface in which adjacent steps are now separated by six-atom wide (1 1 1) terraces. The surface order indicated by LEED appears to be maintained at a quality that is the same as that of the clean Au(2 1 1) surface. Oxygen uptake exceeding $\theta_O = 0.3$ ML diminishes more strongly the intensity of all spots and causes an increase in the background intensity because of the formation of a disordered oxygen layer and eventual disordering of the step structure. No spots characteristic of steps on the surface were observed for $\theta_O = 0.76$–1.0 ML. The strong diffuse intensity and sharp (1 1 1) spots in the LEED pattern for the saturation oxygen coverage indicates a disordered overlayer on top of (1 1 1) terraces.

In addition, LEED was used to investigate the thermally induced 2D ordering of the disordered saturation oxygen monolayer formed on the Au(2 1 1) surface at 300 K. A saturation coverage of oxygen was produced by a 100-L O_3

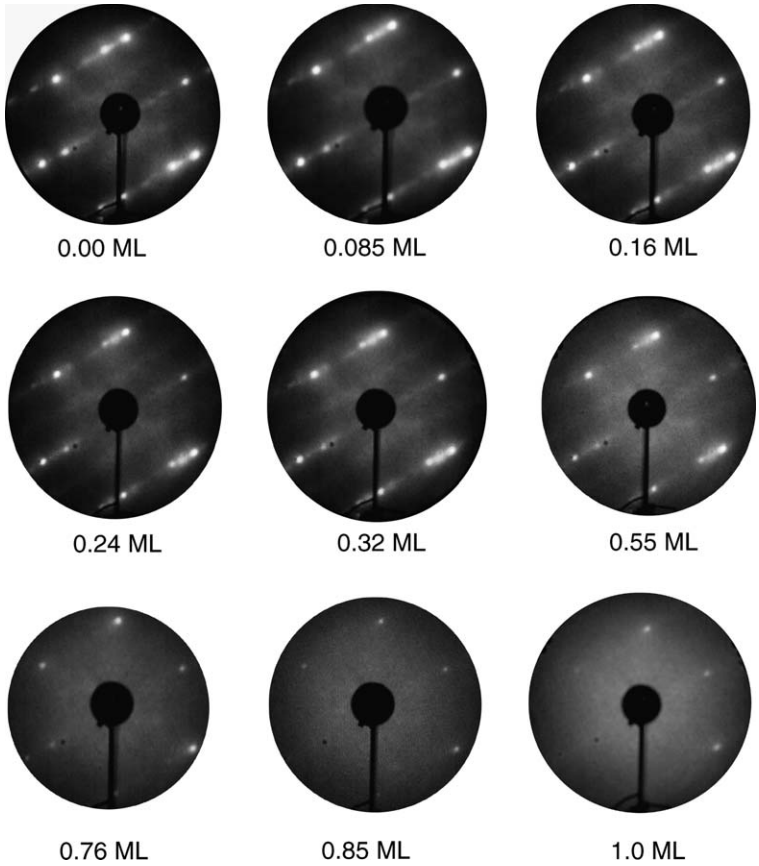

Fig. 7. Photographs of the LEED patterns observed after increasing doses of O_3 on Au(2 1 1) at 300 K. The incident beam energy for LEED was 75 eV. The corresponding oxygen concentration determined by using AES is shown below each LEED photograph.

exposure on the Au(2 1 1) surface at 300 K, and then the crystal was flashed to increasingly higher temperatures. Photographs of the resulting LEED patterns are shown in Fig. 8. Heating the sample also reduces the coverage of oxygen adatoms on the surface and we used AES to quantitatively evaluate this change, and these results are reported below each LEED photograph presented in Fig. 8.

In the upper left-hand corner of Fig. 8, the LEED patterns for a clean Au(2 1 1) surface and a disordered oxygen monolayer with $\theta_O = 0.94$ ML formed on the Au(2 1 1) surface at 300 K are shown for comparison. Flashing the sample briefly to 490 K desorbs a small amount of oxygen as O_2 to leave $\theta_O = 0.74$ ML on the surface, and this removes much of the diffuse background intensity, causes streaking along the $[\bar{1}\,1\,1]$ direction, and produces new spots consistent with step-doubling compared to the clean Au(2 1 1) surface. This surface is much more ordered than was observed at the similar oxygen coverage (0.76 ML) shown in Fig. 7. Heating the crystal to temperatures of 500 or 510 K leaves large coverages of oxygen on the surface and produces increasingly ordered LEED patterns. Flashing to 520 K reduces θ_O to 0.17 ML and leaves only the oxygen that desorbs in a peak in TPD that we associated with step sites. This produces very clear LEED spots at $^1/_6$ of the distance of the (1 1 1) spots along the $[\bar{1}\,1\,1]$ direction because of step doubling. In addition, a new periodicity appears at 1/2 of the distance in the $[\bar{1}\,1\,1]$ direction as faint streaks along the $[\bar{1}\,1\,1]$ direction. This implies an expansion of the unit cell in real space by a factor of two in the $[\bar{1}\,1\,1]$ direction. Heating to 530 K removes this latter periodicity, but evidently even $\theta_O = 0.04$ ML is sufficient to stabilize the step-doubled surface structure. Flashing the crystal to 540 K removes nearly all of the oxygen, and flashing to 600 K does remove all of the oxygen and produces a clean surface. LEED patterns from both of these surfaces show only the pattern characteristic of the clean Au(2 1 1) surface.

In previous related studies, oxygen-induced step-doubling was observed on the Cu(2 1 1) surface along with a transition from monatomic to double-height steps [58,59]. It was reported that oxygen adsorbed without any change in the 2D order at the surface below 250 K, while the surface started to reconstruct and form double-step structures for $\theta_O = 0.05$–0.10 ML at temperatures above 300 K. The reconstruction started initially at the step edges, and the double step was stable up to 800 K.

Disordering at the surface induced by oxygen adsorption has been reported on Au(1 1 1) [20] and Au(1 1 0)-(1×2) [22,34]. The clean Au(1 1 1) surface reconstructs in UHV to a (3×22)-rect. pattern in which each integral-order spot is closely surrounded by a hexagonal cluster of six spots [60]. Low coverages of oxygen adatoms,

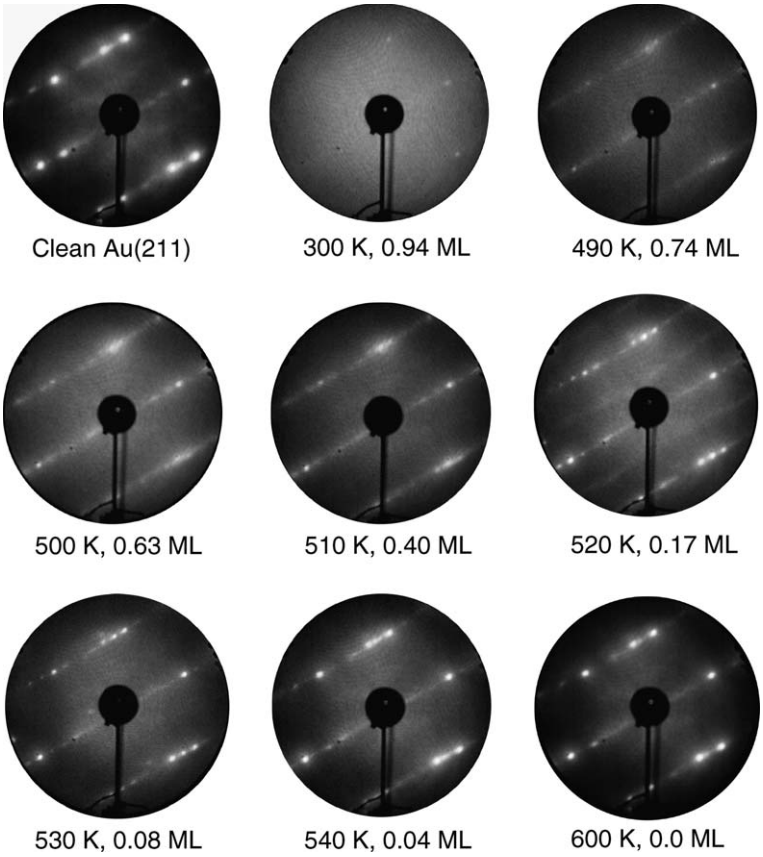

Fig. 8. Photographs of the LEED patterns observed after heating the substrate to several temperatures following dosing 100-L O_3 on Au(2 1 1) at 300 K. The incident beam energy for LEED was 75 eV. The heating temperature and oxygen concentration is shown below each LEED photograph. Heating the crystal induces ordering of the oxygen adlayer and eventually removes oxygen adsorbed on the surface.

$\theta_O < 0.1$ ML, lifted this reconstruction and left only sharp, integral-order spots characteristic of the unreconstructed (1 1 1) surface of a face-centered cubic (fcc) crystal. Higher coverages ($\theta_O \geqslant 0.22$ ML) induced streaks to appear between each of the integral-order spots. At $\theta_O = 1.0$ ML at 300 K, the diffuse background in the LEED pattern became so bright that the substrate LEED spots were nearly obscured. A recent STM study by Min et al. [33] reveals how this reconstruction occurs on the Au(1 1 1) surface. Oxygen adatoms induce a release of Au atoms from the elbows of the (3×22)-rect. structure to form a 'striped soliton-wall' structure at an oxygen coverage of 0.4 ML. Sault et al. [22] and Gottfried et al. [34] also reported a disruption of the long-range order of the Au(1 1 0) surface caused by a saturation coverage of oxygen adatoms.

4. Conclusions

The primary conclusion of our investigations is that the *unstrained* Au(2 1 1) surface does not have a particularly special reactivity associated with the inherent structure of the surface or the step sites that are present on this crystal face for dissociating molecular oxygen (O_2). Our experiments establish that O_2 thermal dissociation is not facile on this surface, and O_2 did not dissociate to produce oxygen adatoms on the stepped Au(2 1 1) surface for large O_2 exposures under UHV conditions or even under high-pressure conditions of 700-Torr O_2 in a reaction cell for 5 min with the sample at 300–450 K. No surface-bound oxygen was detected by TPD or AES following any O_2 exposures investigated. We place a lower limit on the barrier for O_2 dissociative adsorption, E^{diss}, of 27 kcal/mol on the stepped Au(2 1 1) surface.

Ozone (O_3) could be used to produce oxygen adatoms at the Au(2 1 1) surface with a saturation coverage of $\theta_O = 0.90$ ML. TPD revealed the oxygen adsorbed at step sites was bound more tightly than at terrace sites. The oxygen desorption energy, E_d, for the oxygen adsorbed at step sites ($\theta_O \leqslant 0.15$ ML) was estimated by using Redhead analysis to be $E_d = 34$ kcal/mol and for oxygen adsorbed at terrace sites E_d was estimated to be 33 kcal/mol near saturation coverage ($\theta_O = 0.90$ ML). O_2 desorption from the step sites ($\theta_O \leqslant 0.15$ ML) occurs at constant temperature and appears to follow first-order kinetics. Changes observed in LEED during oxygen uptake were interpreted as oxygen-induced step doubling on the Au(2 1 1) surface at low-coverage ($\theta_O = 0.08$–0.17 ML) and extensive disruption of 2D ordering at the surface for saturation coverages of oxygen ($\theta_O \geqslant 0.9$ ML).

In summary, the Au(2 1 1) surface has a reactivity for dissociating O_2 and a chemistry for surface oxygen that quite closely resembles that of the other bulk Au surfaces

that have been investigated to date by surface science experiments, including low-Miller index crystal planes, stepped surfaces, and polycrystalline films. Thus, it is difficult to imagine that the presence of such facets or even high step densities on Au nanoparticles plays a significant part in explaining the novel catalytic activity that has been reported for supported Au nanoparticle catalysts. At the least, this indicates that if such surfaces are important to this chemistry, strain due to the mismatch at the Au-support interface must substantially modify the reactivity of these sites.

Acknowledgements

This work was supported by the Department of Energy, Office of Basic Energy Sciences, Chemical Sciences Division. The authors would like to thank Dr. Michel van Hove for useful discussions concerning our LEED data.

References

[1] B. Hammer, J.K. Nørskov, Nature 376 (1995) 238.
[2] M. Haruta, T. Kobayashi, H. Sano, N. Yamada, Chem. Lett. 2 (1987) 405.
[3] M. Haruta, N. Yamada, T. Kobayashi, S. Iijima, J. Catal. 115 (1989) 301.
[4] S.D. Gardner, G.B. Hoflund, B.T. Upchurch, D.R. Schryer, E.J. Kielin, J. Schryer, J. Catal. 129 (1991) 114.
[5] A. Knell, P. Barnickel, A. Baiker, A. Wokaun, J. Catal. 137 (1992) 306.
[6] M. Haruta, S. Tsubota, T. Kobayashi, H. Kageyama, M.J. Genet, B. Delmon, J. Catal. 144 (1993) 175.
[7] S.D. Lin, M. Bollinger, M.A. Vannice, Catal. Lett. 17 (1993) 245.
[8] S.K. Tanielyan, R.L. Augustine, Appl. Catal. A 85 (1992) 73.
[9] M.A. Bollinger, M.A. Vannice, Appl. Catal. B 8 (1996) 417.
[10] Z.M. Liu, M.A. Vannice, Catal. Lett. 43 (1997) 51.
[11] L. Guczi, D. Horvath, Z. Paszti, L. Toth, Z.E. Horvath, A. Karacs, G. Peto, J. Phys. Chem. B 104 (2000) 3183.
[12] F. Boccuzzi, A. Chiorino, J. Phys. Chem. B 104 (2000) 5414.
[13] J.F. Jia, J.N. Kondo, K. Domen, K. Tamaru, J. Phys. Chem. B 105 (2001) 3017.
[14] Y. Iizuka, T. Tode, T. Takao, K. Yatsu, T. Takeuchi, S. Tsubota, M. Haruta, J. Catal. 187 (1999) 50.
[15] M.M. Schubert, S. Hackenberg, A.C. van Veen, M. Muhler, V. Plzak, R.J. Behm, J. Catal. 197 (2001) 113.
[16] R.J.H. Grisel, B.E. Nieuwenhuys, J. Catal. 199 (2001) 48.
[17] A. Kolmakov, D.W. Goodman, Surf. Sci. 490 (2001) L597.
[18] D.H. Parker, B.E. Koel, J. Vac. Sci. Technol. A. 8 (1990) 2585.
[19] M.A. Lazaga, D.T. Wickham, D.H. Parker, G.N. Kastanas, B.E. Koel, in: J.W. Hightower, S.T. Oyama (Eds.), ACS Symposium Series, ACS, Washington, DC, 1993, p. 90.
[20] N. Saliba, D.H. Parker, B.E. Koel, Surf. Sci. 410 (1998) 270.
[21] J.L. Gland, Surf. Sci. 93 (1980) 487.
[22] A.G. Sault, R.J. Madix, C.T. Campbell, Surf. Sci. 169 (1986) 347.
[23] N.D.S. Canning, D. Outka, R.J. Madix, Surf. Sci. 141 (1984) 240.
[24] V.A. Bondzie, S.C. Parker, C.T. Campbell, J. Vac. Sci. Technol. A 17 (1999) 1717.
[25] S. Evans, E.L. Evans, D.E. Parry, M.J. Tricker, M.J. Walters, J.M. Thomas, Faraday Discuss. 58 (1974) 97.
[26] C. Linsmeier, J. Wanner, Surf. Sci. 454–456 (2000) 305.
[27] J.J. Pireaux, M. Liehr, P.A. Thiry, J.P. Delrue, R. Caudano, Surf. Sci. 141 (1984) 221.
[28] C.R. Aita, N.C. Tran, J. Vac. Sci. Technol. A. 9 (1991) 1498.
[29] L. Maya, M. Paranthaman, T. Thundat, M.L. Bauer, J. Vac. Sci. Technol. B 14 (1996) 15.
[30] B. Koslowski, H.G. Boyen, C. Wilderotter, G. Kastle, P. Ziemann, R. Wahrenberg, P. Oelhafen, Surf. Sci. 475 (2001) 1.
[31] H. Ron, I. Rubinstein, Langmuir 10 (1994) 4566.
[32] X.Y. Deng, B.K. Min, A. Guloy, C.M. Friend, J. Am. Chem. Soc. 127 (2005) 9267.
[33] B.K. Min, X. Deng, D. Pinnaduwage, R. Schalek, C.M. Friend, Phys. Rev. B 72 (2005).
[34] J.M. Gottfried, K.J. Schmidt, S.L.M. Schroeder, K. Christmann, Surf. Sci. 511 (2002) 65.
[35] J.M. Gottfried, K.J. Schmidt, S.L.M. Schroeder, K. Christmann, Surf. Sci. 525 (2003) 184.
[36] M.E. Schrader, Surf. Sci. 78 (1978) L227.
[37] D.D. Eley, P.B. Moore, Surf. Sci. 76 (1978) L599.
[38] P. Legaré, L. Hilaire, M. Sotto, G. Maire, Surf. Sci. 91 (1980) 175.
[39] J.J. Pireaux, M. Chtaib, J.P. Delrue, P.A. Thiry, M. Liehr, R. Caudano, Surf. Sci. 141 (1984) 211.
[40] J.M. Gottfried, N. Elghobashi, S.L.M. Schroeder, K. Christmann, Surf. Sci. 523 (2003) 89.
[41] D.E. King, J. Vac. Sci. Technol. A. 13 (1995) 1247.
[42] A. Krozer, M. Rodahl, J. Vac. Sci. Technol. A. 15 (1997) 1704.
[43] J. Kim, Z. Dohnalek, B.D. Kay, J. Am. Chem. Soc. 127 (2005) 14592.
[44] M. Mavrikakis, P. Stoltze, J.K. Nørskov, Catal. Lett. 64 (2000) 101.
[45] Y. Xu, M. Mavrikakis, J. Phys. Chem. B 107 (2003) 9298.
[46] Z.P. Liu, P. Hu, A. Alavi, J. Am. Chem. Soc. 124 (2002) 14770.
[47] D.W. Blakely, G.A. Somorjai, Surf. Sci. 65 (1977) 419.
[48] J. Wang, B.E. Koel, J. Phys. Chem. A 102 (1998) 8573.
[49] J. Kim, Ph.D., University of Southern California, 2003.
[50] D.A. Syomin, Ph.D., University of Southern California, 2001.
[51] B.D. Kay, K.R. Lykke, J.R. Creighton, S.J. Ward, J. Chem. Phys. 91 (1989) 5120.
[52] D. McIntosh, G.A. Ozin, Inorg. Chem. 15 (1976) 2869.
[53] J.M. Gottfried, K. Christmann, Surf. Sci. 566–568 (2004) 1112.
[54] P.A. Redhead, Vacuum 12 (1962) 203.
[55] D.A. King, Surf. Sci. 47 (1975) 384.
[56] D.H. Parker, M.E. Bartram, B.E. Koel, Surf. Sci. 217 (1989) 489.
[57] D.H. Parker, M.E. Jones, B.E. Koel, Surf. Sci. 233 (1990) 65.
[58] G. Witte, J. Braun, D. Nowack, L. Bartels, B. Neu, G. Meyer, Phys. Rev. B 58 (1998) 13224.
[59] K.A. Thompson, C.S. Fadley, Surf. Sci. 146 (1984) 281.
[60] M.A. Van Hove, R.J. Koestner, P.C. Stair, J.P. Biberian, L.L. Kesmodel, I. Bartos, G.A. Somorjai, Surf. Sci. 103 (1981) 189.